Int. J. Non-Linear Mechanics, Vol. 23, No. 5/6, pp. 369–376, 1988
Printed in Great Britain.

0020 7462/88 $3.00+0.00
Pergamon Press plc

THE TRANSITION FROM PHASE LOCKING TO DRIFT IN A SYSTEM OF TWO WEAKLY COUPLED VAN DER POL OSCILLATORS

TAPESH CHAKRABORTY and RICHARD H. RAND
Department of Theoretical and Applied Mechanics, Cornell University, Ithaca, NY 14853, U.S.A.

(*Received* 14 *October* 1987; *received for publication* 3 *May* 1988)

Abstract—We investigate the slow flow resulting from the application of the two variable expansion perturbation method to a system of two linearly coupled van der Pol oscillators. The slow flow consists of three non-linear coupled odes on the amplitudes and phase difference of the oscillators. We obtain regions in parameter space which correspond to phase locking, phase entrainment and phase drift of the coupled oscillators. In the slow flow, these states correspond respectively to a stable equilibrium, a stable limit cycle and a stable libration orbit. Phase entrainment, in which the phase difference between the oscillators varies periodically, is seen as an intermediate state between phase locking and phase drift. In the slow flow, the transitions between these states are shown to be associated with Hopf and saddle-connection bifurcations.

INTRODUCTION

In this work we shall be concerned with the behavior of two coupled oscillators. We begin by introducing some terminology. We suppose that the outputs of the two oscillators are of the form

$$x_1(t) = R_1(t)\cos(t - \theta_1(t)) \tag{1.1}$$

$$x_2(t) = R_2(t)\cos(t - \theta_2(t)) \tag{1.2}$$

in which $R_i(t)$ represents amplitude modulation and $\theta_i(t)$ represents frequency or phase modulation. We shall define the terms *phase locking*, *phase drift* and *phase entrainment* for two functions of the form (1). Although these definitions can be generalized to apply to a wider class of functions than (1), we shall restrict our attention to such functions since the approximate solutions which we are interested in this work will have this form.

We define the phase difference $\phi(t)$ as

$$\phi(t) = \theta_1(t) - \theta_2(t) \tag{2}$$

Then the functions (1) will be said to be *1:1 phase locked* if $\phi(t)$ is constant. If, on the other hand, the oscillators are running at unequal average frequencies, then $\phi(t)$ will grow unbounded, defining the condition of *1:1 phase drift*. An intermediate situation exists when $\phi(t)$ varies periodically, a condition which we shall call *1:1 phase entrainment* [1].

TWO WEAKLY COUPLED VAN DER POL OSCILLATORS

We shall be interested in the following system of two coupled van der Pol oscillators

$$\frac{d^2x_1}{dt^2} + x_1 - \varepsilon(1 - x_1^2)\frac{dx_1}{dt} = \varepsilon\alpha(x_2 - x_1) \tag{3.1}$$

$$\frac{d^2x_2}{dt^2} + (1 + \varepsilon\Delta)x_2 - \varepsilon(1 - x_2^2)\frac{dx_2}{dt} = \varepsilon\alpha(x_1 - x_2). \tag{3.2}$$

Here $\varepsilon \ll 1$ and Δ and α are parameters. Δ is related to the (small) difference in linearized frequencies, and α represents the strength of the coupling. In a previous work [2], the two variable expansion perturbation method was utilized to obtained an approximate solution to equations (3), valid to order ε:

$$x_1 = R_1(\eta)\cos(t - \theta_1(\eta)) + O(\varepsilon) \tag{4.1}$$

$$x_2 = R_2(\eta)\cos(t - \theta_2(\eta)) + O(\varepsilon) \tag{4.2}$$

where the slow time variable η is given by

$$\eta = \varepsilon t \tag{5}$$

and where the amplitudes R_1 and R_2 and the phase angle $\phi = \theta_1 - \theta_2$ are given by the slow flow on the space M: $R^+ \times R^+ \times S^1$

$$2\frac{dR_1}{d\eta} = -R_1\left[\frac{R_1^2}{4} - 1\right] + \alpha R_2 \sin\phi \tag{6.1}$$

$$2\frac{dR_2}{d\eta} = -R_2\left[\frac{R_2^2}{4} - 1\right] - \alpha R_1 \sin\phi \tag{6.2}$$

$$2\frac{d\phi}{d\eta} = \Delta + \alpha\left[\frac{R_2}{R_1} - \frac{R_1}{R_2}\right]\cos\phi. \tag{6.3}$$

Equations (6) are invariant under the transformation

$$R_1 \to R_2, R_2 \to R_1, \qquad \phi \to \phi - \pi \tag{7}$$

and hence possess the corresponding symmetry. Thus if there is an equilibrium point at (R_1^0, R_2^0, ϕ^0), then there is also one at $(R_2^0, R_1^0, \phi^0 - \pi)$. In order to simplify the following discussion, we shall only talk about half of the system, i.e. if we say that the system (6) contains an equilibrium point (or a periodic orbit), then it actually contains two equilibria (or periodic orbits), the other one being located at the symmetrical position in M under the transformation (7).

RESULTS

Our goal is to classify the various qualitatively distinct behaviors of the system (6) as we change the values of the parameters α and Δ. We summarize here the results obtained in [3].

The system (6) possesses two other symmetries based on invariance under the transformations

$$\alpha \to -\alpha, \qquad \phi \to \phi - \pi, \qquad \text{and} \tag{8.1}$$

$$\Delta \to -\Delta, \qquad \phi \to \pi - \phi. \tag{8.2}$$

Thus it turns out that the qualitative behavior is invariant under both $\alpha \to -\alpha$ and $\Delta \to -\Delta$, and we present our results in the $\alpha^2 - \Delta^2$ parameter plane, see Fig. 1.

The system (6) contains three equilibria in region R in Fig. 1, and one equilibrium elsewhere. Region R can be shown [3] to be bounded by curves having the equation:

$$\Delta^6 + (6\alpha^2 + 2)\Delta^4 + (12\alpha^4 - 10\alpha^2 + 1)\Delta^2 + 8\alpha^6 - \alpha^4 = 0. \tag{9}$$

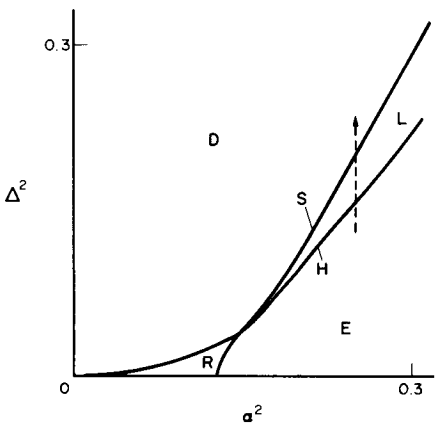

Fig. 1. Bifurcation diagram for the slow flow (6): E = region containing a single stable equilibrium point, L = region containing a stable limit cycle, D = region containing a stable libration orbit, R = region containing three equilibria, H = curve of Hopf bifurcations, S = curve of saddle-connection bifurcations.

In obtaining (9) as well as many of the other results in this work, we used the computer algebra system MACSYMA [4].

The presence of limit cycles in (6) may be investigated by looking for Hopf bifurcations, i.e. by linearizing in the neighborhood of each of the equilibria, and requiring that there exist a pair of pure imaginary eigenvalues. This leads to the curve H in Fig. 1, which can be shown [3] to have the equation:

$$\begin{aligned} &49\Delta^8 + (266\alpha^2 + 238)\Delta^6 + (88\alpha^4 + 758\alpha^2 + 345)\Delta^4 \\ &\quad + (-1056\alpha^6 + 1099\alpha^4 + 892\alpha^2 + 172)\Delta^2 \\ &\quad + (-1152\alpha^8 - 2740\alpha^6 - 876\alpha^4 + 16) = 0. \end{aligned} \tag{10}$$

We showed that stable limit cycles occur in the region lying above curve H in Fig. 1 by using center manifold theory and normal forms [3].

The region L of limit cycles is bounded on the other side by curve S, which we shall show later in this paper to involve saddle-connection bifurcations. As one crosses curve S, the limit cycle becomes a libration orbit, i.e. a closed trajectory in M, along which ϕ increases without bound. The nature of this bifurcation will be discussed in greater detail in the rest of this paper.

The region D of libration orbits is bounded by the curve (9) defining region R. As one crosses from region D into region R, a pair of equilibria are born on the libration orbit, which becomes a non-periodic saddle-connection.

Figure 1 describes the behavior of the slow flow (6). In terms of the original equations (3), region E corresponds to 1:1 phase locking, region L to 1:1 phase entrainment, and region D to 1:1 phase drift. Thus as one moves in the parameter space along the dashed line (corresponding to holding the coupling strength α fixed while increasing the frequency difference Δ), the system (3) passes from phase locking to phase entrainment and then to drift.

THE ENTRAINMENT-DRIFT BIFURCATION

In order to better understand the nature of the bifurcation which results as one crosses from region L to region D in Fig. 1, we display the results of some numerical integrations of the system (6). Figures 2–7 show these results in a portion of the phase space M in which

$$0 \leqslant R_1 \leqslant 4, 0 \leqslant R_2 \leqslant 4, \qquad -\pi \leqslant \phi \leqslant \pi. \tag{11}$$

In each of Figs 2–7, $\alpha^2 = 0.25$, while Δ^2 varies from 0.15 in Fig. 2 (in region E) to 0.21 in Fig. 7 (in region D). Thus this sequence of views corresponds to moving along the dashed line in Fig. 1. Figure 2 shows the asymptotic approach to steady state equilibrium, while Figs 3–7 show only the steady state periodic motions. Between Figs 2 and 3 a Hopf bifurcation has occurred corresponding to passage across curve H in Fig. 1. Figures 3–6 show the gradual increase in size of the limit cycle, and the curve S in Fig. 1 is crossed between Figs 6 and 7.

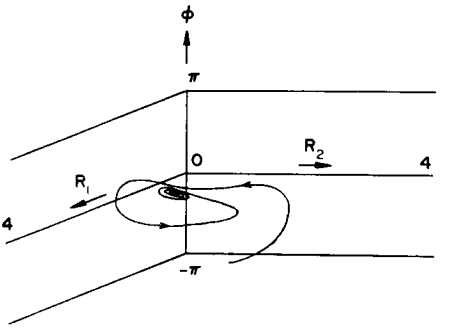

Fig. 2. Numerical integration of equation (6) for $\alpha^2 = 0.25$, $\Delta^2 = 0.15$. Note the asymptotic approach to equilibrium. The labeling of the axes in this figure applies to Figs 3–7 and 9–11.

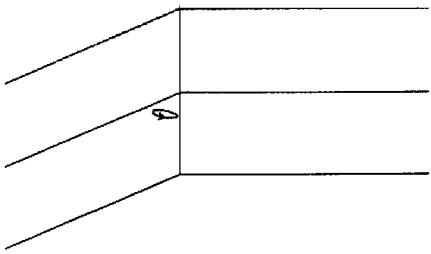

Fig. 3. Limit cycle obtained by numerical integration equations (6) for $\alpha^2 = 0.25$, $\Delta^2 = 0.16$. See Fig. 2 for labeling of axes.

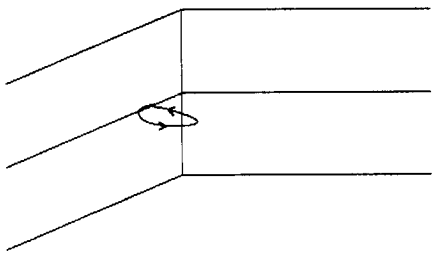

Fig. 4. Limit cycle obtained by numerical integration of equations (6) for $\alpha^2 = 0.25$, $\Delta^2 = 0.17$. See Fig. 2 for labeling of axes.

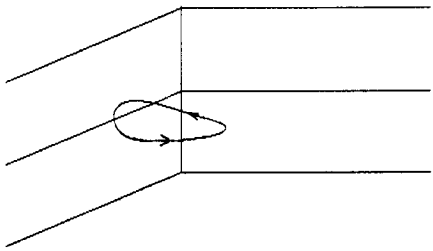

Fig. 5. Limit cycle obtained by numerical integration of equations (6) for $\alpha^2 = 0.25$, $\Delta^2 = 0.185$. See Fig. 2 for labeling of axes.

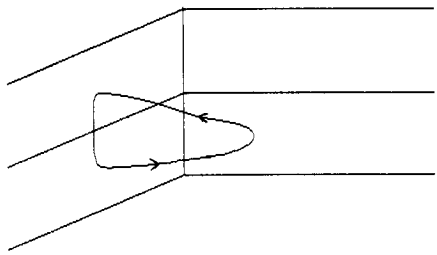

Fig. 6. Limit cycle obtained by numerical integration of equations (6) for $\alpha^2 = 0.25$, $\Delta^2 = 0.20$. See Fig. 2 for labeling of axes.

We note from the numerical integrations that the transition between the limit cycle in Fig. 6 and the libration orbit in Fig. 7 involves a drastic change in the neighborhood of the surface $R_2 = 0$, but little change in the steady state motions elsewhere. In Fig. 6, the portion of the limit cycle near $R_2 = 0$ is a rapid motion at nearly constant R_1 i.e. a jump down in ϕ. In Fig. 7, on the contrary, the libration orbit jumps up in ϕ near $R_2 = 0$.

This observation leads us to examine the behavior of the system (6), when $R_2 = 0$. Since $R_2 = 0$ is a singular surface for the system (6), we change independent variables from η to τ,

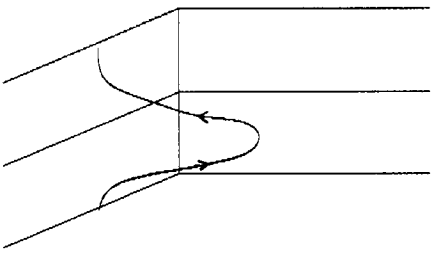

Fig. 7. Libration orbit obtained by numerical integration of equation (6) for $\alpha^2 = 0.25$, $\Delta^2 = 0.21$. Note that this orbit is closed since the planes $\phi = \pi$ and $\phi = -\pi$ are identified with each other. See Fig. 2 for labeling of axes.

where

$$d\tau = \frac{d\eta}{R_2}. \tag{12}$$

This transformation "blows up" the singularity at $R_2 = 0$ ([5], Section 7.2), and while it reparametrizes the motion along the trajectories in M, it does not change the shape of the trajectories. Under (12), the system (6) becomes:

$$2\frac{dR_1}{d\tau} = -R_1 R_2\left[\frac{R_1^2}{4} - 1\right] + \alpha R_2^2 \sin\phi \tag{13.1}$$

$$2\frac{dR_2}{d\tau} = -R_2^2\left[\frac{R_2^2}{4} - 1\right] - \alpha R_1 R_2 \sin\phi \tag{13.2}$$

$$2\frac{d\phi}{d\tau} = \Delta R_2 + \alpha\left[\frac{R_2^2}{R_1} - R_1\right]\cos\phi. \tag{13.3}$$

We note the surface $R_2 = 0$ is an invariant manifold of (13), which becomes when $R_2 = 0$:

$$\frac{dR_1}{d\tau} = 0 \tag{14.1}$$

$$\frac{dR_2}{d\tau} = 0 \tag{14.2}$$

$$2\frac{d\phi}{d\tau} = -\alpha R_1 \cos\phi \tag{14.3}$$

Equations (14) show that R_1 remains constant in time when $R_2 = 0$, and that only ϕ changes. Equation (14.3) has the general solution

$$\tan\left[\frac{\phi}{2} + \frac{\pi}{4}\right] = C e^{-\alpha R_1 \tau/2} \tag{15}$$

where C is an arbitrary constant. Figure 8 shows the flow (14.3) on the ϕ-circle (since R_1 and R_2 are constant). Both Fig. 8 and equation (15) show that as $\tau \to +\infty, \phi \to -\pi/2$, while as $\tau \to -\infty, \phi \to +\pi/2$. This represents the previously referred to jump in ϕ, see Fig. 9.

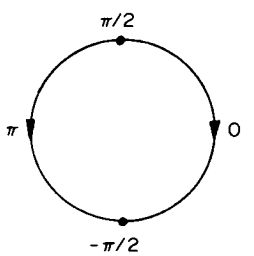

Fig. 8. Flow on the ϕ-circle given by equation (14.3). Arrows show the direction of the flow. Dots represent the equilibria $\phi = \pm\pi/2$

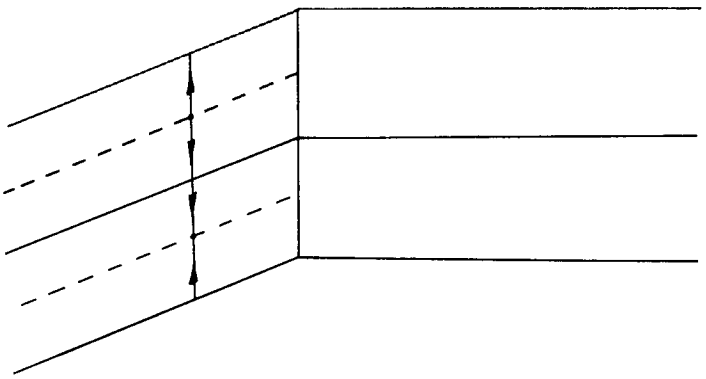

Fig. 9. Flow in the surface $\dot{R}_2 = 0$ given by equation (14). See Fig. 2 for labeling of axes. The dashed lines represent non-isolated equilibria. The lines with arrows represent the flow along R_1 = constant, cf. Fig. 8.

Thus the system (13) has two lines of non-isolated equilibria at $R_2 = 0$, $\phi = +\pi/2$ and at $R_2 = 0$, $\phi = -\pi/2$, shown as dashed lines in Fig. 9. In order to better understand the bifurcation, we consider the nature of these equilibria.

We linearize equations (13) about the equilibrium:

$$R_1 = R_1^0 = \text{any}, \qquad R_2 = 0, \quad \phi = \pm\pi/2 \tag{16}$$

and obtain the variational equations:

$$2\frac{\mathrm{d}}{\mathrm{d}\tau}\delta R_1 = -R_1^0\left[\frac{R_1^{0^2}}{4} - 1\right]\delta R_2 \tag{17.1}$$

$$2\frac{\mathrm{d}}{\mathrm{d}\tau}\delta R_2 = \mp\alpha R_1^0 \delta R_2 \tag{17.2}$$

$$2\frac{\mathrm{d}}{\mathrm{d}\tau}\delta\phi = \Delta\delta R_2 \pm \alpha R_1^0 \delta\phi \tag{17.3}$$

which have the general solution:

$$\begin{bmatrix} \delta R_1 \\ \delta R_2 \\ \delta\phi \end{bmatrix} = k_1\begin{bmatrix} 1 \\ 0 \\ 0 \end{bmatrix} + k_2\begin{bmatrix} 0 \\ 0 \\ 1 \end{bmatrix} e^{\pm R_1^0\alpha\tau/2} + k_3\begin{bmatrix} R_1^{0^2} - 4 \\ \pm 4\alpha \\ -2\Delta/R_1 \end{bmatrix} e^{\mp R_1^0\alpha\tau/2} \tag{18}$$

where the k_i are arbitrary constants. The (1 0 0) eigenvector and accompanying zero eigenvalue are due to the line of non-isolated equilibria and their neutral stability. The (0 0 1) eigenvector corresponds to the flow (15) in the $R_2 = 0$ plane. The motion associated with the third eigenvector permits approach to (or exit from) the equilibrium (16) from (or to) the rest of the space M. Since the equilibria are non-isolated, these eigendirections form a

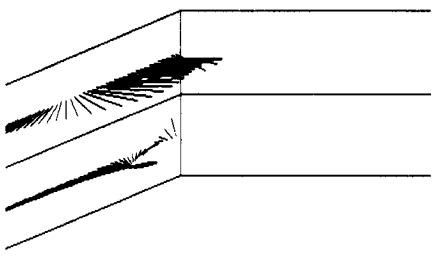

Fig. 10. Eigendirections for the equilibria (16). These surfaces form a stable manifold for the line of equilibria $\phi = \pi/2$ and an unstable manifold for the line of equilibria $\phi = -\pi/2$. See Fig. 2 for labeling of axes.

2-manifold in M, see Fig. 10. These surfaces form a stable manifold for the line of equilibria $\phi = \pi/2$ and an unstable manifold for the line of equilibria $\phi = -\pi/2$.

We return now to the question of the bifurcation from the limit cycle of Fig. 6 to the libration orbit of Fig. 7. In Fig. 11 we superimpose Figs 6 and 7 on the eigenmanifolds of Fig. 10. Figure 11 shows that the bifurcation involves a saddle-connection orbit.

The bifurcation may be further understood by projecting the limit cycle and libration motions on the $\phi - \eta$ cylinder, see Fig. 12.

CONCLUSIONS

It is interesting to compare the results of this study of weakly coupled van der Pol oscillators with those of an earlier study [6] of strongly coupled van der Pol oscillators. In [6] the following system was analyzed by using perturbations to $O(\varepsilon)$:

$$\frac{d^2x_1}{dt^2} + x_1 - \varepsilon(1 - x_1^2)\frac{dx_1}{dt} = \alpha(x_2 - x_1) \tag{19.1}$$

$$\frac{d^2x_2}{dt^2} + (1 + \Delta)x_2 - \varepsilon(1 - x_2^2)\frac{dx_2}{dt} = \alpha(x_1 - x_2). \tag{19.2}$$

Note that equations (19) are of the same same form as equations (3) with $\varepsilon\alpha$ and $\varepsilon\Delta$ replaced by α and Δ respectively. The slow flow resulting from the application of the two variable expansion method to equations (19) has been shown [6] to exhibit phase locking if $\Delta^2 < 2\alpha^2$. If $\Delta^2 > 2\alpha^2$, the system (19) performs a quasiperiodic motion which corresponds to phase drift, see Fig. 13.

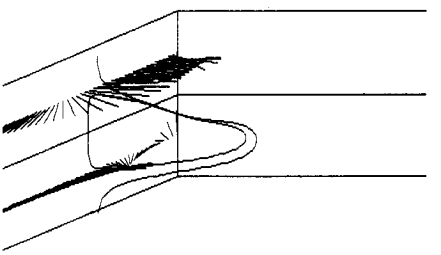

Fig. 11. Superposition of Figs 6, 7, 10. As the limit cycle bifurcates to a libration orbit, there must exist, by continuity, a saddle connection. See Fig. 2 for labeling of axes.

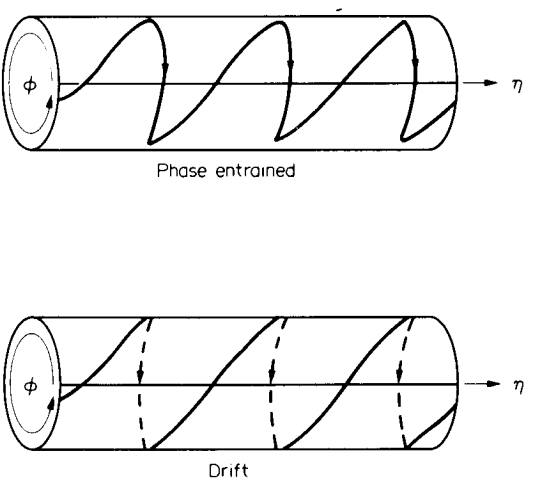

Fig. 12. Projection of the limit cycle of Fig. 6 and the libration orbit of Fig. 7 onto the ϕ–η cylinder. The top and bottom of the cylinder represent $\phi = \pi/2$ and $\phi = -\pi/2$, respectively. The limit cycle (corresponding to phase entrainment) lies entirely on the front face of the cylinder, while the libration motion (corresponding to drift) winds completely around the cylinder. In the case of the phase entrained motion, $\phi(\eta)$ is periodic, while for the drift case, $\phi(\eta)$ becomes unbounded as η goes to infinity.

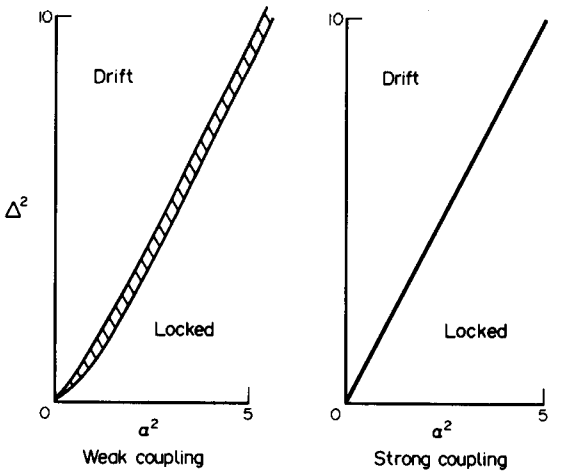

Fig. 13. Comparison of the dynamics of the weakly coupled system (3) studied in this work with the strongly coupled system (19) studied in [6]. The shaded region represents phase entrainment.

For large values of α and Δ, the Hopf curve (10) in the weakly coupled case may be written (keeping highest order terms only):

$$49\Delta^8 + 266\alpha^2\Delta^6 + 88\alpha^4\Delta^4 - 1056\alpha^6\Delta^2 - 1152\alpha^8 = 0 \tag{20}$$

which may be factored to give

$$(\Delta^2 - 2\alpha^2)(\Delta^2 + 4\alpha^2)(7\Delta^2 + 12\alpha^2)^2 = 0. \tag{21}$$

Thus the Hopf curve (10) approaches $\Delta^2 = 2\alpha^2$ as Δ and α approach infinity, in agreement with the strongly coupled case (19). Numerical simulation of the slow flow system (6) reveals that the saddle connection curve S of Fig. 1 also approaches this limit. See Fig. 13, in which the behavior of systems (3) and (19) is compared.

In conclusion, we see that the approximate solution for the weakly coupled case studied in this paper exhibits a gradual transition from phase locking to phase drift, separated by an intermediate region of phase entrainment. The comparable transition in the strongly coupled case is sharp. As noted in [3] and [6], numerical simulations of the original systems (3) and (19) show that the actual transition is in fact gradual.

REFERENCES

1. W. L. Keith and R. H. Rand, 1:1 and 2:1 phase entrainment in a system of two coupled oscillators. *J. math. Biol.* **20**, 133–152 (1984).
2. R. H. Rand and P. J. Holmes, Bifurcation of periodic motions in two weakly coupled Van der Pol oscillators. *Int. J. Non-linear Mech.* **15**, 387–399 (1980).
3. T. Chakraborty, Bifurcation analysis of two weakly coupled Van der Pol oscillators. Doctoral thesis, Cornell University (1986).
4. R. H. Rand, *Computer Algebra in Applied Mathematics: An Introduction to MACSYMA*. Research Notes in Mathematics No. 94. Pitman, Belmont, CA (1984).
5. J. Guckenheimer and P. Holmes, *Non-linear Oscillations, Dynamical Systems and Bifurcations of Vector Fields*. Applied Math. Sciences Vol. 42. Springer, New York (1983).
6. D. W. Storti and R. H. Rand, Dynamics of two strongly coupled Van der Pol oscillators. *Int. J. Non-linear Mech.* **17**, 143–152 (1982).